Assessment of Myocardial Oxidative Metabolic Reserve with Positron Emission Tomography and Carbon-11 Acetate

C. Gregory Henes, Steven R. Bergmann, Mary Norine Walsh, Burton E. Sobel, and Edward M. Geltman

Cardiovascular Division, Washington University School of Medicine, St. Louis, Missouri

We have previously demonstrated that positron emission tomography (PET) with [^{11}C]acetate allows noninvasive regional quantification of myocardial oxidative metabolism. To assess the metabolic response of normal myocardium to increased work (oxidative metabolic reserve), clearance of myocardial ^{11}C activity after administration of [^{11}C]acetate i.v. was measured with PET in seven normal subjects at rest and during dobutamine infusion. At rest, clearance of ^{11}C was monoexponential and homogeneous. The rate constant of the first phase of ^{11}C clearance, k_1, averaged 0.054 ± 0.014 min^{-1} at a rate-pressure produce (RPP) of 7329 ± 1445 mmHg × bpm. During dobutamine infusion, RPP increased by an average of 141% to 17 493 ± 3582 mm Hg × bpm. Clearance of ^{11}C became biexponential and remained homogeneous. k_1 averaged 0.198 ± 0.043 min^{-1} with a mean coefficient of variation of 16%. k_1 and RPP correlated closely ($r = 0.91$; $p < 0.001$), and the slope of the k_1/RPP relation remained consistent in all subjects (1.48 ± 0.42). These findings suggest that PET with [^{11}C] acetate and dobutamine stress may provide a promising approach for evaluation of regional myocardial oxidative metabolic reserve in patients with cardiac diseases of diverse etiologies and for assessment of the efficacy of interventions designed to enhance the recovery of metabolically comprised myocardium.

J Nucl Med 30: 1489–1499, 1989

Acute syndromes reflecting coronary artery disease (CAD) are characterized by an imbalance between regional myocardial oxygen supply and oxygen demand at rest or with stress, an imbalance that may be manifest clinically as stable angina, variant angina, unstable angina, or myocardial infarction. Unfortunately, however, diagnosis may be limited by difficulties in quantifying regional myocardial oxygen consumption ($M\dot{V}O_2$). $M\dot{V}O_2$ can be measured directly at the time of cardiac catheterization, but regional differences are difficult to quantify because of an admixture of coronary venous drainage. Furthermore, widely applicable, noninvasive procedures have not been available. Coronary angiography provides descriptions of epicardial coronary vascular lesions, but does not measure the adequacy of regional perfusion which is influenced not only by the geometry of individual lesions but also by the number of lesions in sequence and their length, the presence of collateral flow, and myocardial compressive forces (among other factors). Measures of regional ventricular function extrapolated from radionuclide ventriculograms, contrast ventriculograms or echocardiograms are affected not only by regional perfusion but also by preload, afterload, autonomic tone, and circulating catecholamines.

Positron emission tomography (PET) is a promising tool for characterizing regional myocardial perfusion and oxidative metabolism (*1*). Studies with tracers of metabolism of fatty acid [carbon-11- (^{11}C) labeled palmitate] (*2,3*) and glucose [fluorine-18- (^{18}F) labeled fluorodeoxyglucose ([^{18}F]FDG)] (*4*) have delineated striking changes in patients with coronary artery disease and cardiomyopathy. However, quantification of overall regional myocardial oxidative metabolism based on analysis of the behavior of these tracers is limited because their uptake and clearance depends upon arterial substrate content, sensitivity of uptake to the hormonal environment, and competition among multiple metabolic pathways influencing the intracellular fates of each (*5–10*). Measures of glycolytic flux have been useful in distinguishing viable from nonviable myocardium.

Received Jan. 17, 1989; revision accepted Apr. 12, 1989.

For reprints contact: C. Gregory Henes, MD, Cardiovascular Division, Box 8086, Washington University School of Medicine, 660 S. Euclid Ave, St. Louis, MO 63110.

However, they cannot differentiate aerobic from anaerobic glycolysis.

With ischemia, a backdiffusion of initially extracted but unmetabolized tracers such as [^{11}C]palmitate may lead to overestimates of beta oxidation (*8,9*). As we have recently shown, with ischemia and reperfusion the pattern of substrate use changes rapidly (*7*). Thus, estimates of overall regional oxidative metabolism with either glucose or fatty acid as the sole tracer do not delineate regional rates of myocardial oxidative metabolism or oxygen consumption.

Because metabolic flux through the tricarboxylic acid (TCA) cycle is tightly coupled to oxidative metabolism in the heart, we hypothesized that its delineation would provide accurate estimates of regional myocardial oxygen consumption. Studies with experimental animals in our laboratory demonstrated that tricarboxylic acid cycle flux could be traced with either [^{14}C]acetate or [^{11}C]acetate and that flux through the cycle correlated closely with myocardial oxygen consumption (*11–13*). In isolated perfused rabbit hearts, we found that the correlation between TCA cycle flux, measured by the oxidation of labeled acetate to labeled CO_2, and oxygen consumption was close over a wide range of physiologic and metabolic conditions (*11*). In closed-chest dogs studied with PET, close associations between oxidation of extracted acetate to labeled CO_2, myocardial clearance of ^{11}C activity, and myocardial oxygen consumption over a wide range of cardiac work loads were demonstrated (*12*). The correlation between [^{11}C]acetate clearance and $M\dot{V}O_2$ was unaffected by the pattern of carbohydrate and/or fatty acid substrate use (*13*).

In pilot studies in normal human subjects we delineated homogeneous extraction of [^{11}C] acetate throughout the myocardium with monoexponential clearance when the subjects were at rest (*14*). In patients with myocardial infarction, uptake was reduced in ischemic zones and clearance of extracted tracer was diminished, indicative of diminished regional myocardial oxygen consumption (*14*). Because the capacity of myocardium to augment oxidative metabolism in response to increased physiologic demand (metabolic reserve) is not necessarily parallel to the capacity for augmentation of regional perfusion (myocardial perfusion reserve) the present study was performed to determine whether clearance of [^{11}C]acetate was augmented in myocardium of normal subjects under conditions of increased cardiac work, paralleling the known, homogeneous increase in regional myocardial oxygen consumption under these circumstances. Our objectives were: (a) to determine the feasibility of measuring regional alterations in oxidative metabolism in human subjects; (b) to determine whether the close relationship between [^{11}C] acetate clearance and myocardial oxygen consumption observed in animals was evident also in normal human subjects; and (c) to define the extent of myocardial metabolic reserve apparent in normal human subjects in response to marked augmentation of cardiac contractility.

METHODS

The protocol used was approved by the Washington University Human Studies Committee. Informed written consent was obtained from all subjects. The study population comprised seven healthy male volunteers aged 21 to 34 yr without prior history of cardiac disease, chest pain, hypertension, or cardiac arrhythmias, or ECG criteria of cardiac disease. All subjects were studied in the fasted state. A polyurethane mold of the subject's upper torso was formed to maximize patient comfort and minimize patient motion during the study. A 25-cm, 17-gauge polyethylene catheter was placed in an antecubital vein for injection of tracer and a short 18-gauge catheter placed in the contralateral forearm for sampling venous blood. Subjects were positioned within the tomograph so that the heart was centered within the instrument's field of view with the aid of positioning light beams and indelible markings to ensure accurate repositioning.

Collection of Data

Subjects were studied in Super PETT I, a whole-body, time-of-flight positron emission tomography permitting acquisition of list mode data sufficient for the reconstruction of seven transaxial slices with a slice thickness of 1.14 cm and a center-to-center slice separation of 1.5 cm (*15*). Operated in high resolution, time-of-flight mode, the scanner has an effective sensitivity of 170,000 cps/μCi/cc. Data were reconstructed with an effective full width half maximum resolution of 13.5 mm. At the beginning of each study, to correct for photon attenuation, a 12-min transmission scan using a ^{68}Ge/^{68}Ga source was acquired. Proper positioning of the patient was verified by review of transmission tomograms prior to the administration of radiotracers. Subsequently, to permit visualization of the blood pool, 40 mCi to 50 mCi of oxygen-15-labeled carbon monoxide (C^{15}O) were administered by inhalation. After 30 to 60 sec to allow equilibration with the blood pool, data were collected for 300 sec in list mode. Five to 10 minutes thereafter, [^{11}C]acetate (0.4 mCi/kg) was administered as a bolus intravenously, and data acquired for 30 min in list mode. The patient was removed from the scanner and permitted to rest for ~45 min, after which an incremental infusion of dobutamine was initiated as described below. After a maximal steady-state infusion of dobutamine had been established, C^{15}O and [^{11}C]acetate were administered again. Imaging was repeated as in the baseline study.

Total reconstructed counts per study averaged $15–30 \times 10^6$. The approximate average cts/slice/scan was 3.5 ± 10^6. Radioactivity was reconstructed into "PET" counts which are linearly proportional to true count rate. At similar count rates to those observed in human subjects after [^{11}C]acetate administration, phantom studies yielded a scale factor of ~100 PET cts/sec/μCi.

Infusion of Dobutamine

Infusion of dobutamine was employed to increase myocardial work. We utilized dobutamine rather than exercise to

augment myocardial oxygen consumption because: (a) dobutamine has been shown to increase cardiac work safely in patients with CAD (*16–21*); (b) dobutamine provides a continuous homogeneous stress over the 30 min required for [^{11}C] acetate imaging, in contrast to exercise which may not be sustainable at a constant, high workload for 30 min; (c) exercise performed during acquisition of tomographic data may lead to artifacts because of motion of the thorax.

Infusion of dobutamine began with a dose of 5 μg/kg/min. Every 5 min, the infusion rate was increased by 5 μg/kg/min up to a maximum dose of 20 μg/kg/min or until one of the following endpoints had been reached: heart rate >80% of maximum predicted heart rate for age; blood pressure >200/110 mmHg or <90/60; or an absolute decrease in blood pressure ≥20 mmHg; occurrence of chest pain; ST-segment depression ≥2 mm or ST-segment elevation ≥1 mm; occurrence of significant atrial or ventricular arrhythmias. If a clinical endpoint was reached at a given infusion rate, the infusion was stopped for 5 min and then restarted at the preceding infusion rate. This procedure was continued until an infusion rate could be maintained for at least 5 to 7 min without eliciting a clinical endpoint. Once the maximum tolerable infusion rate had been established, the infusion was maintained at that level for the entire duration of the second [^{11}C]acetate scan. Heart rate and blood pressure were monitored every 15 min at rest, every min during incremental infusions of dobutamine, and at 3 min intervals during the steady state infusion of dobutamine. The ECG was monitored continuously oscilliscopically and recorded at baseline and every 3 min with infusions. Blood was sampled for measurement of substrates (glucose, free fatty acids, acetate) at baseline and at the beginning, midpoint, and conclusion of tomographic data collection performed during infusion of dobutamine. Glucose was assayed using a commercially available enzymatic kit (Behring Diagnostics, La Jolla, CA). Analysis of free fatty acids and acetate were performed as previously described (*22,23*).

In order to measure true blood radioactivity, in one subject studied at rest, venous blood was withdrawn every minute for the first 4 min after administration of tracer, then every 2 min for 16 additional minutes, and then every 4 min until the end of the data acquisition. Total ^{11}C radioactivity, $^{11}CO_2$, and non-$^{11}CO_2$ radioactivity were measured in each sample as previously described (*12*).

Analysis of Data

The data collected after administration of [^{11}C]acetate were reconstructed in two ways. Each tomograph slice was represented as a 128 × 128 voxel array. Data acquired between 3 min and 8 min after administration of tracer were reconstructed as composite images used solely for placement of regions of interest (ROI). Data were reconstructed also into 20 serial 90-sec frames commencing at the time of injection of [^{11}C]acetate. To assess the regional homogeneity of myocardial metabolic function, multiple contiguous regions of interest (each encompassing a volume of 1.3 cm^3) were placed around the circumference of two or more ventricular slices with the use of an interactive computer system. In addition, a single large global region of interest encompassing the entire myocardium was placed on each tomographic reconstruction to determine average tracer kinetics.

The data acquired after the inhalation of C^{15}O were reconstructed into a single composite reconstruction for each tomographic level. These reconstructions were used for placement of regions of interest in the left atrial blood pool so that the ^{11}C radioactivity in arterial blood could be determined.

The radioactivity within each region of interest was determined for each time point and corrected for physical decay of the tracer. Time-activity curves were obtained from each region of interest and analyzed with a multi-exponential least squares curve fitting algorithm. Data from the first 120 to 180 sec were excluded because they are influenced by continuing uptake of tracer and spillover of radioactivity from the blood pool. Curves were fit beginning with the time of onset of the most rapid decrease in counts after the initial peak, generally between 180 and 270 sec after injection of tracer. Time-activity curves were fitted using a Marquardt nonlinear least-squares fitting algorithm which weights data points inversely proportional to the time of their occurrence. This accounts for the decreasing reliability of count statistics due to tracer clearance and radioactive decay. Although all curves were initially intended to be fitted by a multi-exponential function, as detailed below, curves obtained under resting conditions only conformed to a monoexponential fit. Because clearance from the blood pool was rapid with values declining by 85 to 90% from peak values within 3 min, correction of myocardial radioactivity for spillover from the blood pool was not required. The ^{11}C turnover rate constant was defined as the coefficient k_1 from the equation:

$$Q = A_1 e^{-k_1 t}$$

for monoexponential curves and:

$$Q = A_1 e^{-k_1 t} + A_2 e^{-k_2 t}$$

for biexponential curves where,

Q = myocardial ^{11}C activity,
A_1 and A_2 = constants (y intercepts),
k_1 and k_2 = myocardial turnover rate constants, and t = time.

The half-time ($t_{1/2}$) of the rapid phase of clearance of ^{11}C radioactivity was defined as $\ln 2/k_1$.

Results of previous studies from our laboratory have shown that the myocardial turnover rate constant k_1 assessed after the i.v. injection of [^{11}C]acetate correlates closely with myocardial oxygen consumption $M\dot{V}O_2$ measured directly by arterial and coronary sinus measurements in intact dogs (n = 33) (*12,13*). Because normal ranges of $M\dot{V}O_2$ are available from prior catheterization studies in human subjects, we did not feel that coronary sinus catheterization was necessary or justified in the present study. Accordingly, for purposes of comparison to determinants of myocardial oxygen requirements (rate pressure product) $M\dot{V}O_2$ was estimated for each defined region of interest based on the relationship between $M\dot{V}O_2$ and k_1 that had been delineated in studies of dogs.

Preparation of Tracers

$C_{15}O$ and [^{11}C]acetate were prepared as previously described (*11,24,25*). Purity of [^{11}C]acetate was evaluated by HPLC for every preparation and generally exceeded 99.5% with specific radioactivity of [^{11}C]acetate > 1 Ci/mmol.

STATISTICS

Results are reported as means ± s.d. Differences between studies performed at rest and during dobutamine infusion were assessed with paired t-tests. Linear regression was calculated by the least-squares method; $p < 0.05$ was considered to be significant.

RESULTS

Hemodynamics

Hemodynamics recorded at rest and in response to infusion of dobutamine are indicated in Table 1. The results reported for dobutamine-stress reflect an average of values obtained during the steady-state infusion while tomographic data were being collected. The rate pressure product (RPP) [heart rate × systolic blood pressure], an index of global myocardial work, was calculated for all subjects. RPP increased by at least 73% in all subjects during infusion of dobutamine, with the increase averaging 141 ± 50% ($p < 0.001$ versus studies at rest). The response to dobutamine varied substantially from subject to subject. Some demonstrated predominant increases in heart rate and others prominent increases in systolic blood pressure. The doses of dobutamine employed during steady state infusions during tomographic data collections are indicated in Table 1. The maximal target dose of 20 μg/kg/min was achieved in five of the seven subjects. In the remaining two subjects, the dose was limited by the blood pressure response. RPP remained constant during the steady-state infusion of dobutamine with a mean coefficient of variation of 4.5%.

All subjects tolerated the tomographic procedures well. In no subject was there an adverse response to infusion of dobutamine or administration of tracer.

Tomographic Observations

Typical images at four levels of the ventricle from a normal subject acquired at rest are displayed in Figure 1. The data incorporated in these reconstructions represent radioactivity recorded between 3 and 8 min after injection of [^{11}C]acetate. These data were reconstructed without blood-pool subtraction or spillover correction. In all subjects accumulation of [^{11}C]acetate appeared homogeneous at all tomographic levels of the heart recorded at rest and after infusion of dobutamine.

Quantitative Analysis of Tomographic Data

The radioactivity assessed in the cardiac blood pool declined rapidly in all subjects at rest and after infusion or dobutamine (Fig. 2). By 180 sec after administration of tracer, blood-pool radioactivity had fallen to < 21% of peak radioactivity in all subjects. At the time of the first point employed for the analysis of clearance of ^{11}C radioactivity from myocardium, < 15% of the radioactivity in the myocardial regions of interest was attributable to radioactivity emanating from the cardiac blood pool. Rate constants for k_1 derived from spillover-corrected clearance curves calculated as previously reported (12) differed by < 5% from rate constants from uncorrected curves. Thus, no corrections were necessary for spillover of radioactivity from the blood pool

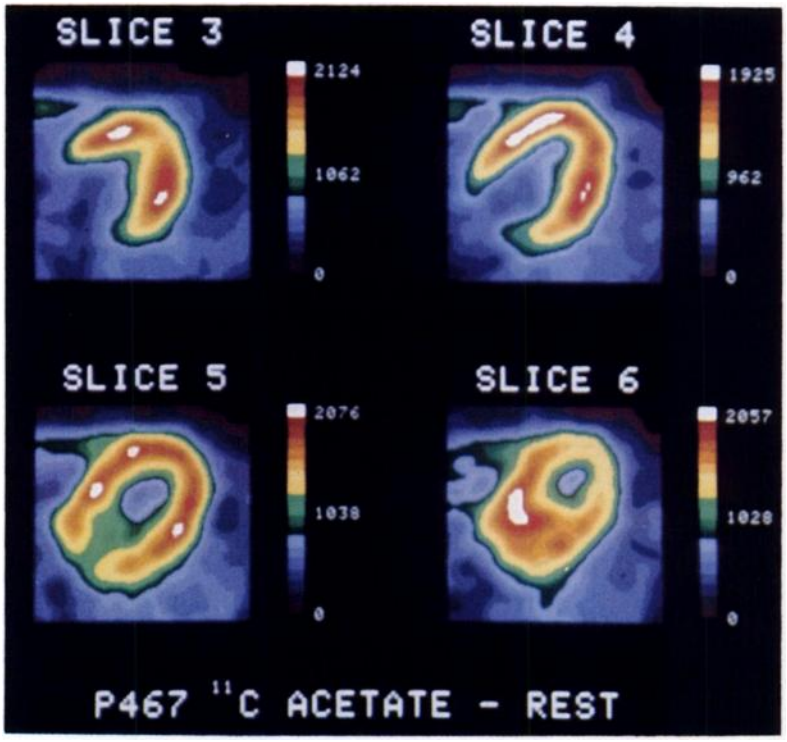

FIGURE 1
Four transverse tomographic reconstructions from data acquired 3 to 8 min after the i.v. infusion of [^{11}C]acetate at the following levels: Upper left—base; upper right—midventricle; bottom left—papillary muscle; bottom right—apex. The top of each image represents anterior, the left of each image represents the patient's right. Accumulation of [^{11}C]acetate was homogeneous throughout all levels of the ventricle.

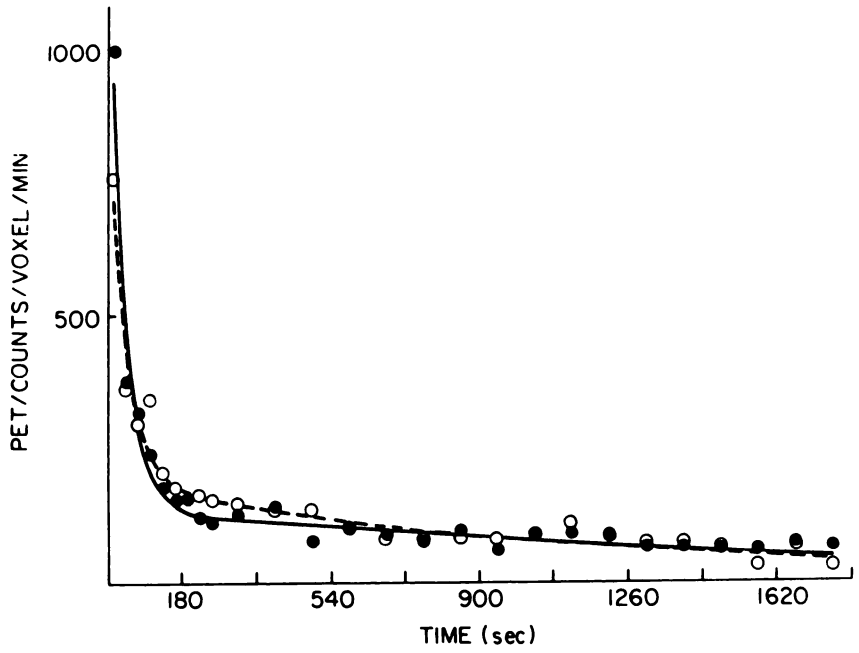

FIGURE 2
Time-activity curve representing radioactivity in the left atrial blood pool at rest (closed circles, solid line) and during infusion of dobutamine (open circles, broken line) after the bolus i.v. injection of [^{11}C]acetate in a human subject. Clearance of radioactivity from the blood pool was rapid. Within 180 sec after injection, blood-pool radioactivity was <21% of peak activity. Dobutamine did not appreciably alter the time course of blood-pool clearance.

to the myocardium for characterization of myocardial clearance of ^{11}C radioactivity. In one subject, sequential samples of venous blood were obtained and analyzed for total ^{11}C radioactivity, $^{11}CO_2$, and non-$^{11}CO_2$ after administration of [^{11}C]acetate intravenously. Total ^{11}C radioactivity decreased rapidly to <10% of peak within several minutes of the injection of tracer (Fig. 3), and then remained relatively constant for the duration of the scan with the proportion of $^{11}CO_2$ increasing. Non-CO_2 radioactivity, representing unmetabolized [^{11}C] acetate (and potentially labeled intermediates, other than $^{11}CO_2$, later in the scan) represented < 5% of that present immediately after administration of tracer. Because first-pass extraction of [^{11}C]acetate is ~30%, the contribution of continued [^{11}C]acetate uptake to total myocardial activity is negligible after the first 2–4 min of the scan (*12*).

In all normal subjects, clearance of ^{11}C radioactivity from the heart was monoexponential at rest. After infusion of dobutamine, clearance became biexponential in six of seven subjects (Fig. 4). The rate constants k_1 (and corresponding $t_{1/2}$) of [^{11}C]acetate in each subject calculated from data acquired at rest and during infusion of dobutamine are indicated in Table 1. Each value recorded in the table represents an average from two to four regions of interest, each encompassing the entire myocardium in a single tomographic reconstruction from contiguous ventricular levels. k_1 increased from 0.054 ± 0.014 min^{-1} to 0.198 ± 0.043 min^{-1} during infusion of dobutamine with a corresponding decrease in $t_{1/2}$ from 13.4 ± 3.5 to 3.7 ± 1.1 min ($p < 0.001$ for each comparison). The rate constant, k_2, for the second component of the biexponential curve was several orders of magnitude lower than that for k_1, indicating that the second phase of [^{11}C]acetate clearance was extremely slow (Table 1). Clearance was homogenous throughout the myocardium at rest and after

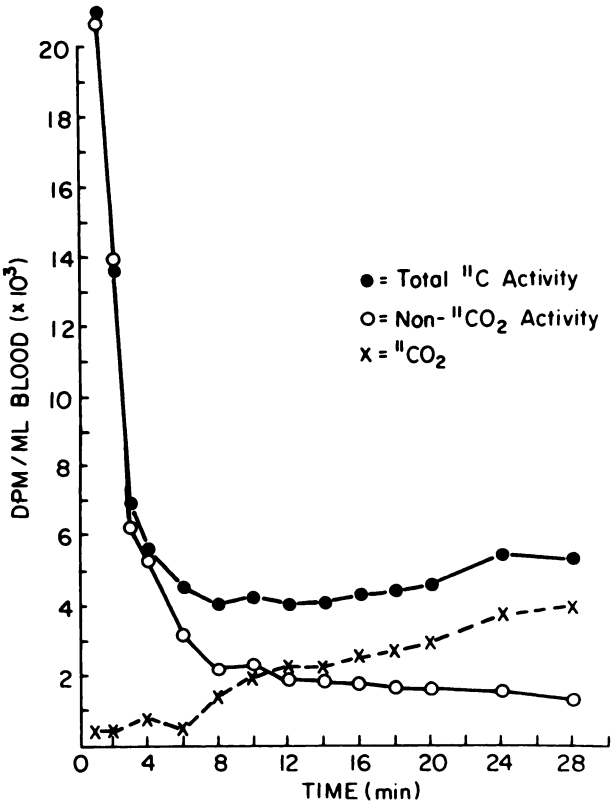

FIGURE 3
Sequential venous blood radioactivity obtained from one subject at rest after the intravenous administration of [^{11}C] acetate. Total blood ^{11}C radioactivity declined rapidly, and non-$^{11}CO_2$ activity (representing predominantly [^{11}C]acetate) represented a relatively minor fraction.

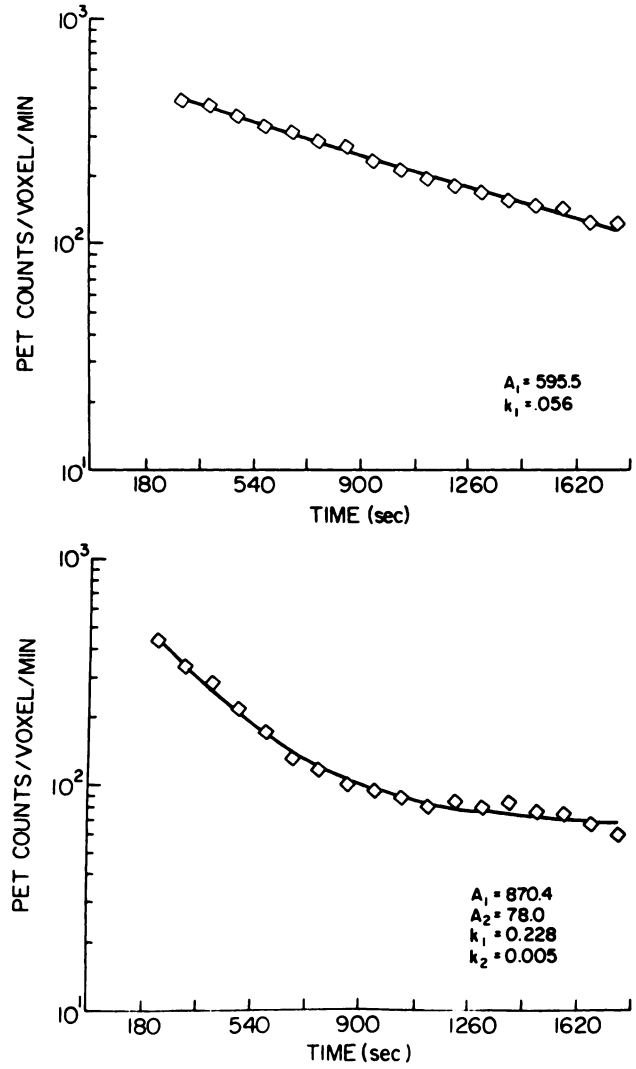

FIGURE 4
Upper panel: time-activity curve representing ^{11}C-radioactivity in the left ventricular myocardium in a study performed at rest. Clearance is monoexponential. Lower panel: time-activity curve from the same region of interest in the same patient with data acquired during the infusion of dobutamine. The rate of clearance of radioactivity in the early phase is increased. The overall curve is biexponential. A_1 and A_2 represent the y intercept of the fast (k_1) and slow (k_2) component of the time-activity curve.

infusion of dobutamine. Regional values for the rate constant k_1 are indicated in Table 2. Values for each myocardial zone represent the mean from 3 to 12 regions of interest from one to four ventricular levels for each patient.

The relationship between k_1 and rate pressure product for the seven subjects studied is depicted in Figure 5. The rate constant, k_1, correlated closely with rate pressure product ($r = 0.91$, $p < 0.001$) over a wide range of conditions. When data were plotted relating basal and dobutamine stress values for each subject (Fig. 6) it was clear that the relationship between global myocardial work, reflected by rate pressure product, and global myocardial oxygen consumption, reflected by the myocardial clearance of ^{11}C, was consistent from patient to patient. The slope of each individual's k_1/RPP relationship was remarkably similar ($1.48 \pm 0.42 \times 10^{-5}$ mm Hg^{-1}).

Calculated values for $M\dot{V}O_2$ are shown in Table 1. Estimated $M\dot{V}O_2$ in normal human subjects at rest averaged 0.92 ± 0.38 μmol/g/min. During infusion of dobutamine $M\dot{V}O_2$ increased markedly and homogeneously.

As shown in Figure 7, the relationship between k_1 and the rate pressure product for the seven subjects studied plus five normal subjects reported previously (*14*), who were studied only at rest, is concordant with the corresponding relationship in hearts of experimental animals (*12,13*).

Infusion of dobutamine had no appreciable effect on concentrations of glucose in plasma, but did increase plasma free fatty acid concentrations markedly needs, presumably because of increased lipolysis resulting from beta-adrenergic stimulation (Table 3). Plasma concentrations of acetate increased slightly and transiently during infusion of dobutamine in two subjects.

DISCUSSION

The data obtained indicate that the uptake and clearance of [^{11}C]acetate in hearts of normal human subjects is homogeneous throughout left ventricular myocardium under baseline conditions and with increased cardiac work induced by the intravenous administration of dobutamine. Furthermore, increases in the rate of clearance of [^{11}C]acetate parallel and are proportional to increases in cardiac work.

In experimental animals the kinetics of clearance of ^{11}C from myocardium provide an accurate measure of tricarboxylic acid (TCA) cycle flux and of myocardial oxygen consumption (*11–13*). Results from studies with isolated perfused hearts and intact dogs indicate that oxidation of acetate to CO_2 in the TCA cycle parallels myocardial oxygen consumption and that clearance of ^{11}C from myocardium mirrors the production of $^{11}CO_2$ from labeled acetate. These relationships pertain over a wide range of myocardial mechanical loading conditions and substrate availability. Thus, assessment of clearance of ^{11}C appears to obviate some of the difficulties inherent in the analysis of the kinetics of other metabolic tracers such as [^{11}C]palmitate and [^{18}F]FDG for which kinetics are affected markedly by plasma concentrations of substrate, backdiffusion, distribution in multiple intracellular pools, and diverse metabolic fates (*5–10*). Because proportional utilization of fatty acid, glucose, and lactate change with ischemia (*7*), assessment of total myocardial oxidative capacity

TABLE 1
Hemodynamics and Kinetics of ^{11}C Radioactivity*

Subject	HR (min^{-1})	Systolic BP (mm Hg)	RPP (mm Hg·min^{-1})	k_1 (min^{-1})	$t_{½}$ (min)	Calculated MVO_2 (μmol/g/min)	k_2 (min^{-1})	Infusion (μg/kg/min)
				Rest				
429	83	126	10 458	0.059	11.9	1.05	—	
444	68	106	7 228	0.078	9.0	1.58	—	
452	62	117	7 227	0.035	19.7	0.39	—	
457	57	116	6 647	0.045	15.7	0.67	—	
466	59	105	6 253	0.056	12.5	0.97	—	
467	57	107	6 287	0.047	15.0	0.72	—	
469	67	108	7 200	0.060	11.5	1.08	—	
Mean ± s.d.	65 ± 9	112 ± 8	7 328 ± 1445	0.054 ± 0.014	13.5 ± 3.5	0.92 ± 0.38		
				Dobutamine				
429	148	148	21 815	0.231	3.0	5.83	2.47×10^{-5}	20
444	107	172	18 447	0.233	3.0	5.89	—	20
452	82	203	16 671	0.116	6.0	2.64	1.17×10^{-10}	10
457	124	178	22 083	0.223	3.1	5.61	1.18×10^{-5}	15
466	109	152	16 565	0.222	3.1	5.58	1.90×10^{-5}	20
467	83	173	14 405	0.183	3.8	4.50	3.03×10^{-5}	20
469	81	155	12 467	0.175	4.0	4.28	2.67×10^{-11}	20
Mean ± s.d.	105 ± 25	169 ± 19	17 493 ± 3582†	0.198 ± 0.043†	3.7 ± 1.1†	4.90 ± 1.19†	$1.43 \pm 1.26 \times 10^{-5}$	

* Heart (HR); blood pressure (BP); rate pressure product (RPP); myocardial turnover rate constant (k_1); clearance half-time ($t_{½}$); calculated myocardial oxygen consumption (MVO_2) and infusion rate of dobutamine for each subject. ^{11}C kinetics were averages over large regions of interest encompassing the entire ventricular myocardium on three to four transverse reconstructions. Hemodynamic data during dobutamine represent an average of those recorded during PET data collections. Dashed line (—) indicates a value for k_2, the slower biexponential component, could not be identified by the curve fitting procedure.

† $p < 0.005$ compared with rest study.

TABLE 2
Regional Myocardial Turnover Rate Constants (k_1)*

Subject	Septal	Anterior	Lateral	Posterior	Global regions	COV (%)
			Rest			
429	0.060 ± 0.004	0.060 ± 0.001	0.057 ± 0.004	0.053 ± 0.006	0.059 ± 0.001	7.2
444	0.100 ± 0.025	0.072 ± 0.021	0.081 ± 0.020	0.116 ± 0.015	0.078 ± 0.002	28.0
452	0.034 ± 0.004	0.032 ± 0.007	0.032 ± 0.005	0.036 ± 0.007	0.035 ± 0.002	16.2
457	0.049 ± 0.004	0.043 ± 0.004	0.044 ± 0.003	NA	0.045 ± 0.000	10.3
466	0.060 ± 0.006	0.059 ± 0.003	0.054 ± 0.005	0.052 ± 0.009	0.056 ± 0.002	11.0
467	0.050 ± 0.003	0.048 ± 0.005	0.046 ± 0.003	0.047 ± 0.003	0.047 ± 0.002	8.3
469	0.060 ± 0.003	0.060 ± 0.003	0.062 ± 0.004	0.055 ± 0.002	0.060 ± 0.002	6.4
Mean ± s.d.	0.059 ± 0.020	0.053 ± 0.013	0.054 ± 0.015	0.060 ± 0.028	0.054 ± 0.014	12.5 ± 7.6
			Dobutamine			
429	0.249 ± 0.034	0.277 ± 0.013	0.279 ± 0.026	0.251 ± 0.070	0.231 ± 0.008	13.0
444	0.227 ± 0.046	0.224 ± 0.046	0.238 ± 0.052	NA	0.233 ± 0.062	20.3
452	0.096 ± 0.007	0.090 ± 0.004	0.092 ± 0.006	NA	0.116 ± 0.009	6.7
457	0.243 ± 0.049	0.256 ± 0.038	0.265 ± 0.018	0.257 ± 0.021	0.223 ± 0.011	14.0
466	0.250 ± 0.063	0.236 ± 0.047	0.238 ± 0.032	0.220 ± 0.017	0.222 ± 0.009	19.0
467	0.182 ± 0.059	0.238 ± 0.046	0.211 ± 0.033	0.204 ± 0.013	0.183 ± 0.011	23.5
469	0.196 ± 0.023	0.185 ± 0.032	0.203 ± 0.038	0.175 ± 0.030	0.175 ± 0.010	16.2
Mean ± s.d.	0.206 ± 0.055	0.215 ± 0.062	0.218 ± 0.062	0.221 ± 0.034	0.198 ± 0.043	16.1 ± 5.5

* Coefficient of variation (COV); NA indicates posterior region could not be visualized in any tomographic slice. Minor discrepancies between the ability to visualize posterior myocardium during rest and dobutamine studies in an individual subject reflect slight changes in cardiac postion and size during inotropic stimulation.

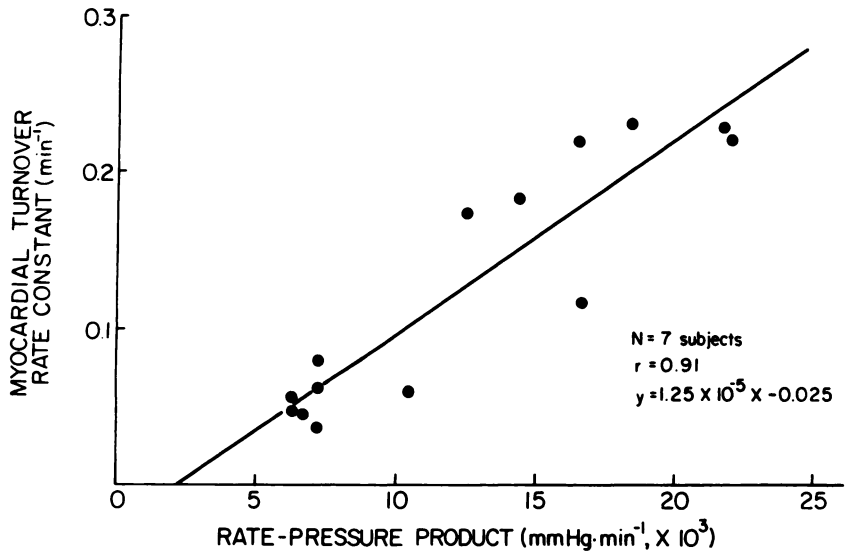

FIGURE 5
Correlation between the myocardial turnover rate constant (k_1) measured by PET after the i.v. administration of [^{11}C]acetate and the rate-pressure product with data acquired at rest and during infusion of dobutamine in seven normal subjects. The correlation was close over a wide range of cardiac loading conditions.

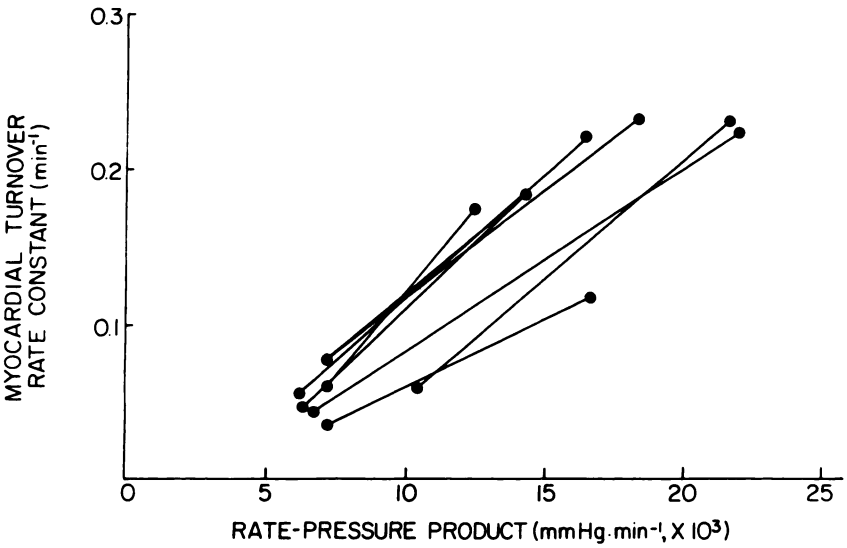

FIGURE 6
The relationship between the myocardial turnover rate constant (k_1) and rate-pressure produce with data acquired before and during infusion of dobutamine for individual subjects.

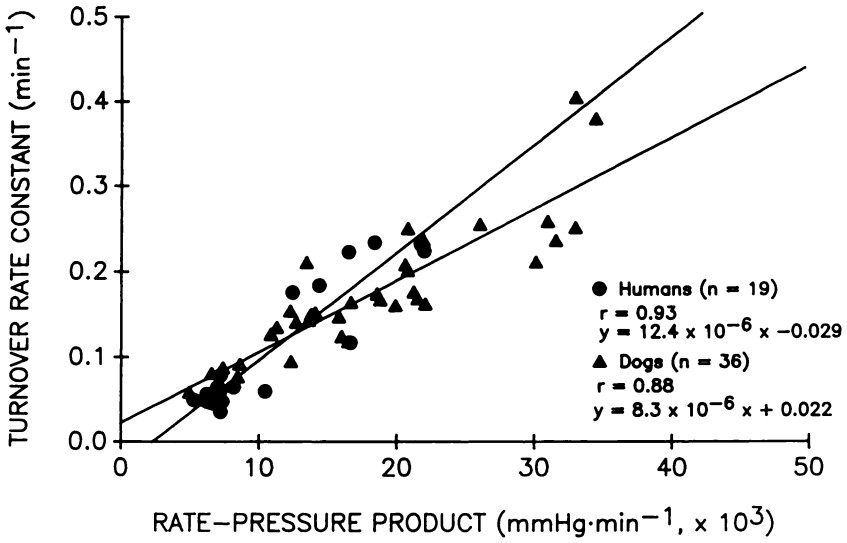

FIGURE 7
Correlation of the myocardial turnover rate constant (k_1) and the rate-pressure product for data acquired in human subjects and data acquired previously from experimental animals in our laboratory (*12,13*) under a variety of cardiac loading conditions. The two regression lines are not statistically different.

TABLE 3
Plasma Substrate Levels

	Rest acetate scan	Acetate scan during dobutamine		
	Midpoint	Start	Midpoint	Conclusion
Glucose (m*M*)	4.8 ± 0.4	4.9 ± 0.1	4.7 ± 0.2	4.6 ± 0.4
Free fatty acids (μ*M*)	522 ± 243	906 ± 370	822 ± 128	829 ± 103
Acetate (μ*M*)	106 ± 23	121 ± 16	203 ± 83	145 ± 16

is not possible by analysis of metabolism of any one of them alone.

Both oxidative glucose metabolism and beta oxidation of fatty acids result in the production of acetyl-CoA which subsequently undergoes oxidative metabolism in the mitochondria through the tricarboxylic acid cycle. Thus, the tricarboxylic acid flux reflects overall oxidation of substrate regardless of origin in long-chain fatty acid or carbohydrate. The close relationship between $M\dot{V}O_2$ and acetate clearance is unaltered by conditions of ischemia, hypoxia, and altered substrate availability (*11–13*). Thus, measurement of ^{11}C clearance with PET after injection of [^{11}C]acetate permits noninvasive, regional assessment of myocardial oxidative metabolism.

Dobutamine exerts potent positive inotropic effects and can activate beta-1, beta-2, and alpha-1 adrenoreceptors (*26,27*). It improves myocardial performance in patients with reduced cardiac output resulting from acute coronary syndromes, cardiomyopathy, or valvular heart disease (*27*). It has been used for pharmacologic stress testing (*16–21*) because it increases myocardial oxygen demand by increasing both heart rate and blood pressure without unduly increasing the incidence of cardiac arrhythmias. In experimental animals, dobutamine alters the distribution of coronary blood flow to zones distal to coronary stenoses and induces regional abnormalities of left ventricular wall motion, wall thickening, and ventricular performance in animals with significant coronary stenoses (*28–34*). Regional alterations of left ventricular wall motion (*16,18–20*) and of the distribution of ^{201}Tl (*17*) occur with dobutamine stress in human subjects with coronary artery disease.

We used dobutamine to induce pharmacologic stress so that regional myocardial metabolic reserve could be characterized in this study because it increases myocardial oxygen demand without the need for exercise. The continuous stimulus required to provide a homogeneous metabolic stress over a 30-min interval would not be readily accomplished with exercise stress because most patients would not have sufficient endurance. Furthermore, exercise would be likely to give rise to significant image artifacts because of motion. Atrial pacing was not selected because of its invasive nature and because the extent of myocardial stress that can be induced with atrial pacing is modest (*35*). Varying degrees of atrioventricular block are encountered often before the RPP is increased maximally when pacing is employed.

The uptake and clearance of [^{11}C]acetate was found to be homogeneous in normal subjects at rest and with pharmacologic stress. The early phase of clearance of ^{11}C increased proportionally to increasing global cardiac work as measured by the rate-pressure product. The increase in the rate of clearance of ^{11}C from myocardium was spatially uniform. After dobutamine, the kinetics of clearance became biexponential. The rate constant of the second component of the clearance curve was extremely low. Late clearance represented a very small proportion of initially extracted tracer. If whole myocardial regions of interest were used for time-activity analysis, it was possible, under some circumstances, to define biexponential clearance of ^{11}C radioactivity from the heart. However parameters estimated in this manner had a standard error of ~ 40–200% compared to an error of 1.5–3% using the monoexponential fit. When biexponential fits were possible in subjects at rest, A_2 averaged 4% of A_1, and k_2 averaged < 0.1% of k_1. Thus, it is probable that clearance is biexponential at rest in humans but the second component is obscured by the relatively slow clearance of the first component at rest and is also obscured by statistical noise. In several subjects studied previously for up to 60 min after administration of tracer, no biexponential component of clearance could be seen (*14*). In addition, it should be noted that the clearance of the second component even after dobutamine is essentially infinite. Thus, for clinical applications, fitting of the early portion of all time-activity curves to a monoexponential simplifies the computational analysis and is accurate and valid under most circumstances, especially for interrogation of small regions of interest. Carbon-11 acetate entering the slowly turning over pool most likely represents incorporation of [^{11}C]acetate into amino acids (glutamate, glutamine, and aspartate) or into lipid pools (*11,36,37*).

Because the RPP correlates closely with global myocardial oxygen consumption (determined invasively) in animals (*12,13*) and patients (*38–40*) and because k_1 correlates closely with myocardial oxygen consumption measured directly in animals, the present results suggest that the rate of clearance of ^{11}C from the myocardium in man provides a noninvasive measure of regional $M\dot{V}O_2$. Values of $M\dot{V}O_2$ estimated in patients ranged

from 0.92 ± 0.38 μmol/g/min at rest to 4.90 ± 1.19 μmol/g/min with infusion of dobutamine. These estimated values are somewhat lower than those that have been measured invasively in human subjects (*38–40*). The discrepancy may reflect interspecies differences in the numerical relation of k_1 to $M\dot{V}O_2$ (*11–13,41*).

Clinical Implications

Noninvasive assessment of regional myocardial oxygen consumption has considerable potential utility for the evaluation of patients with cardiac disease. It should permit assessment of the physiologic significance of coronary stenoses by determination of the metabolic consequences of physiologic stress in patients with obstructive coronary lesions of questionable physiologic significance. In addition, it should provide estimates of tissue viability and metabolic reserve in patients with coronary artery disease, cardiomyopathy, valvular heart disease, and other processes manifested by abnormalities of regional or global function. It should facilitate objective noninvasive assessments of the potential benefit of therapeutic interventions and improve the selection of patients likely to benefit from diverse procedures including coronary artery bypass grafting, valve replacement, and cardiac transplantation.

ACKNOWLEDGMENTS

The authors thank Theron Baird and Colleen Schaab, RN for technical assistance; Dave Marshall, Jim Bakke, and the staff of the Washington University Medical Center Cyclotron for tracer preparation; and Joyce Kalayeh and Becky Leonard for secretarial assistance.

This work was supported in part by National Heart, Lung and Blood Institute, grant HL17646, Specialized Center of Research in Ischemic Heart Disease.

REFERENCES

1. Bergmann SR, Fox KAA, Geltman EM, Sobel BE. Positron emission tomography of the heart. *Prog Cardiovasc Dis* 1985; 28:165–194.
2. Sobel BE, Geltman EM, Tiefenbrunn AJ, et al. Improvement of regional myocardial metabolism after coronary thrombolysis induced with tissue-type plasminogen activator or streptokinase. *Circulation* 1984; 69:983–990.
3. Geltman EM, Smith JL, Beecher D, Ludbrook PA, Ter-Pogossian MM, Sobel BE. Altered regional myocardial metabolism in congestive cardiomyopathy detected by positron tomography. *Am J Med* 1983; 74:773–785.
4. Marshall RC, Tillisch JH, Phelps ME, et al. Identification and differentiation of resting myocardial ischemia and infarction in man with positron computed tomography, ^{18}F-labeled fluorodeoxyglucose and N-13 ammonia. *Circulation* 1983; 67:766–778.
5. Schelbert HR, Henze E, Schon HR, et al. C-11 palmitate for the noninvasive evaluation of regional myocardial fatty acid metabolism with positron computed tomography. III. In vivo demonstration of the effects of substrate availability on myocardial metabolism. *Am Heart J* 1983; 105:492–504.
6. Schelbert HR, Henze E, Sochor H, et al. Effects of substrate availability on myocardial C-11 palmitate kinetics by positron emission tomography in normal subjects and patients with ventricular dysfunction. *Am Heart J* 1986; 111:1055–1064.
7. Myears DW, Sobel BE, Bergmann SR. Substrate use in ischemic and reperfused canine myocardium: quantitative considerations. *Am J Physiol: Heart Circ Physiol* 1987; 253:H107–H114.
8. Fox KAA, Abendschein D, Ambos HD, Sobel BE, Bergmann SR. Efflux of metabolized and nonmetabolized fatty acid from canine myocardium. Implications for quantifying myocardial metabolism tomographically. *Circ Res* 1985; 57:232–243.
9. Rosamond TL, Abendschein DR, Sobel BE, Bergmann SR, Fox KAA. Metabolic fate of radiolabeled palmitate in ischemic canine myocardium: Implications for positron emission tomography. *J Nucl Med* 1987; 28:1322–1329.
10. Merhige ME, Ekas R, Mossberg K, Taegtmeyer H, Gould KL. Catecholamine stimulation, substrate competition, and myocardial glucose uptake in conscious dogs assessed with positron emission tomography. *Circ Res* 1987; 61:II-124-II-129.
11. Brown MA, Marshall DR, Sobel BE, Bergmann SR. Delineation of myocardial oxygen utilization with carbon-11 labeled acetate. *Circulation* 1987; 76:687–696.
12. Brown MA, Myears DW, Bergmann SR. Noninvasive assessment of canine myocardial oxidative metabolism with carbon-11 acetate and positron emission tomography. *J Am Coll Cardiol* 1988; 12:1054–1063.
13. Brown MA, Myears DW, Bergmann SR. Validity of estimates of myocardial oxidative metabolism with carbon-11-acetate and positron emission tomography despite altered patterns of substrate utilization. *J Nucl Med* 1989; 30:187–193.
14. Walsh MN, Brown MA, Henes CG, et al. Estimation of regional myocardial oxidative metabolism by positron emission tomography with carbon-11-acetate in patients [Abstract]. *Circulation* 1988; 78(II):599.
15. Ter-Pogossian MM, Ficke DC, Yamamoto M, Hood JT. Super PETT I: a positron emission tomograph utilizing photon time-of-flight information. *IEEE Trans Med Imag* 1982; 3:179–187.
16. Freeman ML, Palac R, Mason J, et al. A comparison of dobutamine infusion and supine bicycle exercise for radionuclide cardiac stress testing. *Clin Nucl Med* 1984; 19:251–255.
17. Mason JR, Palac RT, Freeman ML, et al. Thallium scintigraphy during dobutamine infusion: nonexercise-dependent screening test for coronary disease. *Am Heart J* 1984; 107:481–485.
18. Meyer SL, Curry GC, Donsky MS, Twieg DB, Parkey RW, Willerson JT. Influence of dobutamine on hemodynamics and coronary blood flow in patients with and without coronary artery disease. *Am J Cardiol* 1976; 38:103–108.
19. David D, Lang RM, Borow KM. Clinical utility of exercise, pacing, and pharmacologic stress testing for the noninvasive determination of myocardial contractility and reserve. *Am Heart J* 1988; 116:235–247.
20. Berthe C, Pierard LA, Hiernaux M, et al. Predicting the extent and location of coronary artery disease in acute myocardial infarction by echocardiography during dobutamine infusion. *Am J Cardiol* 1986; 58: 1167–1172.
21. Mannering D, Cripps T, Leech G, et al. The dobuta-

mine stress test as an alternative to exercise testing after acute myocardial infarction. *Br Heart J* 1988; 59:521–526.
22. Bergmann SR, Carlson E, Dannen E, Sobel BE. An improved assay with 4-(2-thiazlylaso)-resorcinol for non-esterified fatty acids in biological fluids. *Clinica Chimica Acta* 1980; 104:53–63.
23. Bergmeyer HU, Mollering H. Acetate. In: Bergmeyer HU, ed. *Methods of enzymic analysis.* Weinheim: Verlag-Chemie, 1984; 628–639.
24. Welch MJ, Ter-Pogossian MM. Preparation of short half-lived radioactive gases for medical studies. *Rad Res* 1968; 36:580–587.
25. Pike VW, Eakins MN, Allan RM, Selwyn AP. Preparation of [1-^{11}C]acetate—an agent for the study of myocardial metabolism by positron emission tomography. *Int J Appl Radiat Isot* 1982; 33:505–512.
26. Tuttle RR and Mills J. Dobutamine: development of a new catecholamine to selectively increase cardiac contractility. *Circ Res* 1975; 36:185–196.
27. Ruffolo RR. Review: the pharmacology of dobutamine. *Am J Med Sci* 1987; 294:244–248.
28. Willerson JT, Hutton I, Watson JT, Platt MR, Templeton GH. Influence of dobutamine on regional myocardial blood flow and ventricular performance during acute and chronic myocardial ischemia in dogs. *Circulation* 1976; 53:828–833.
29. Tuttle RR, Pollock GD, Todd G, MacDonald B, Tust R, Dusenberggy W. The effect of dobutamine on cardiac oxygen balance, regional blood flow, and infarction severity after coronary artery narrowing in dogs. *Circ Res* 1977; 41:357–364.
30. Warltier DC, Zyvoloski M, Gross GJ, Hardman HF, Brooks HL. Redistribution of myocardial blood flow distal to a dynamic coronary arterial stenosis by sympathomimetic amines. *Am J Cardiol* 1981; 48:269–279.
31. Lanzer P, Garrett J, Lipton M, et al. Quantitation of regional myocardial function by cine computed tomography: pharmacologic changes in wall thickness. *J Am Coll Cardiol* 1986; 8:682–692.
32. Buda AJ, Zotz RJ, Gallagher KP. The effect of inotropic stimulation on normal and ischemic myocardium after coronary occlusion. *Circulation* 1987; 76:163–172.
33. Fung AY, Gallagher KP, Buda AJ. The physiologic basis of dobutamine as compared with dipyridamole stress interventions in the assessment of critical coronary stenosis. *Circulation* 1987; 76:943–951.
34. McGillen MJ, DeBoe SF, Friedman HZ, Mancini GBJ. The effects of dopamine and dobutamine on regional function in the presence of rigid coronary stenoses and subcritical impairments of reactive hyperemia. *Am Heart J* 1988; 115:970–977.
35. Grover-McKay M, Schelbert HR, Schwaiger M, et al. Identification of impaired metabolic reserve by atrial pacing in patients with significant coronary artery stenosis. *Circulation* 1986; 74:281–292.
36. Neurohr KH, Barrett EJ, Shulman RS. *In vivo* carbon-13 nuclear magnetic resonance studies of heart metabolism. *Proc Natl Acad Sci USA* 1983; 80:1603–1607.
37. Malloy CR, Sherry AD, Jeffrey FMH. Carbon flux through citric acid cycle pathways in perfused heart by ^{13}C NMR spectroscopy. *FEBS Lett* 1987; 212:58–62.
38. Kitamura K, Jorgensen CR, Gobel FL, Taylor HL, Wang Y. Hemodynamic correlates of myocardial oxygen consumption during upright exercise. *J Appl Physiol* 1972; 32:516–522.
39. Nelson RR, Gobel FL, Jorgensen CR, Wang K, Wang Y, Taylor HL. Hemodynamic predictors or myocardial oxygen consumption during static and dynamic exercise. *Circulation* 1974; 50:1179–1189.
40. Gobel FL, Nordstrom LA, Nelson RP, Jorgensen CR, Wang Y. The rate-pressure product as an index of myocardial oxygen consumption during exercise in patients with angina pectoris. *Circulation* 1978; 57:549–556.
41. Buxton DB, Schwaiger M, Nguyen A, Phelps ME, Schelbert HR. Radiolabeled acetate as a tracer of myocardial tricarboxylic acid cycle flux. *Circ Res* 1988; 63:628–634.